Micromechanical model of interface damage accumulation in fibrous composite

Volodymyr I. Kushch
vkushch@bigmir.net

Abstract

Two micromechanical, representative unit cell type models of fibrous composite are applied to simulate explicitly an onset and development of scattered local damage in the form of matrix-to-fiber interface debonding. The first one is based on the analytical, multipole expansion type solution of the problem for multiple interacting inclusions with interface arc cracks by means of complex potentials. The second, finite element model employs cohesive zone model of interface. Computer simulation of interface damage accumulation by means of these models has been performed. It has been shown that the developed models provide detailed analysis of the progressive debonding phenomena including the interface crack cluster formation, overall stiffness reduction and induced anisotropy of the effective elastic moduli of composite. Application of the statistical theory of extreme values to the progressive damage description has been discussed. Based on observation that the statistics of peak interface stress in disordered fibrous composite follows a Frechet-type asymptotic rule, the macro level model of initial stage of damage accumulation in fibrous composite is suggested.

1 Introduction

Interface debonding is a common damage in composite materials [1] that greatly affects its mechanical behavior and must be taken into account in the predictive models. The scattered damage starts at micro level by developing the multiple interface cracks between the fibers and matrix. These cracks tend to form the chain-like clusters, oriented predominantly across the loading direction, then coalesce and give rise a macro-level failure of composite. This and other analogous *collective* phenomena cannot be captured by simple models. Their description implies (a) realistic structure model, capable to mimic the fiber arrangement and the local damage events, (b) accurate evaluation of the local stress concentrations and (c) adequate interface damage model. Among a variety of models proposed to predict damage accumulation, the progressive damage models involving the variables related to measurable manifestations of damage (interface debonding, transverse matrix cracks, delamination size, etc.) are considered as the most promising tool [2].

A few publications are available in literature where an explicit simulation of progressive interface debonding were performed for the realistic structure model. In [3], Voronoi cell finite element model was used to study decohesion at multiple fiber interface. There, debonding is accommodated by cohesive zone model (CZM), where the normal and tangential tractions are expressed in terms of interface separation. In [5], simulation of progressive debonding in fibrous composite has been performed based on the multiple fiber-matrix contact problem with CZM option. A similar approach was suggested recently in [6] and [11] who implemented the CZM by means of interface finite elements. Recently, an accurate an-

alytical solution have been obtained [4] of the 2D elasticity problem for a fibrous composite with arc interface cracks.

The primary goal of this paper is a comparative study of two micromechanical models. A more challenging outcome of these simulations consists in developing the consistent macro level theory of composite strength. To this end, we need to link the micro structure parameters to the peak local stress statistics and micro damage onset and accumulation rate. As an example, a simple continuum theory of interface damage accumulation in fibrous composite has been suggested.

2 Model of composite bulk

We consider the representative unit cell (RUC) model of fibrous composite. The model is periodic, with the period a along the axes Ox_1 and Ox_2 (Fig. 1). It contains N randomly arranged, aligned in x_3-direction circular fibers of radius R. The whole composite bulk is obtained by translating RUC in two orthogonal directions. The fiber volume content is $c = N\pi R^2/a^2$. The geometry shown in Figs 1 and 4 was generated with aid of the molecular dynamics code [7].

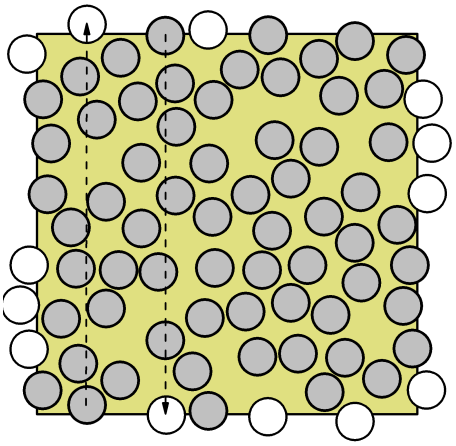

Fig. 1. RUC model of fibrous composite

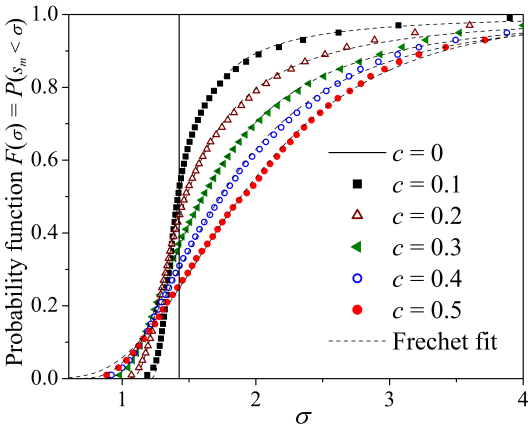

Fig. 2. Empiric probability function of the peak interface stress s_m: an effect of fiber volume content

This model was studied by several investigators under assumption that the matrix and fibers are perfectly bonded along the interfaces L_q, $q = 1, 2, ..., N$. We consider more general case by assuming the part L_{qb} of interface L_q to be perfectly bonded and the part $L_{qs} = L_q \setminus L_{qb}$ to be separated in the course of loading.

The plane strain 2D elasticity problem ($u_3 = 0$) is stated on this geometry model. Both the matrix and fiber materials are assumed isotropic and linearly elastic. The in-plane displacement vector in the matrix material with a shear modulus μ_0 and Poisson ratio ν_0 is denoted as $\mathbf{u}_0$; $\mathbf{u}_q$, μ_1 and ν_1 refer to displacement, shear modulus and Poisson ratio of q-th fiber, respectively. The displacement vector obeys the Lamé equation, the small strain ε and stress σ tensors yield the Hooke's law. The macroscopically uniform stress field in the composite bulk is assumed. This implies constancy of the macroscopic strain $\langle\varepsilon\rangle$ and stress $\langle\sigma\rangle$ tensors defined as

$$\langle\varepsilon\rangle = \frac{1}{2A}\int_{\partial A} (\mathbf{n}\otimes\mathbf{u} + \mathbf{u}\otimes\mathbf{n})\, dL; \quad \langle\sigma\rangle = \frac{1}{A}\int_{\partial A} \mathbf{r}\otimes(\sigma\cdot\mathbf{n})\, dL; \tag{1}$$

respectively, where ∂A is an outer boundary of RUC and $A = a^2$ is the cell area. Eqs. (1) involve only the *observable* quantities, i.e. tractions and displacements at outer boundary ∂A. Importantly, they hold true (in contrast to the volume averaging-based definition) for the composites with imperfect interfaces.

Either $\langle\varepsilon\rangle$ or $\langle\sigma\rangle$ can be taken as a governing parameter of the problem. Periodicity of the material structure results in quasi-periodicity of the displacement and periodicity of the local strain and stress fields:

$$\mathbf{u}\left(\mathbf{r}+a\mathbf{e}_i\right)=\mathbf{u}\left(\mathbf{r}\right)+a\left\langle\varepsilon\right\rangle\cdot\mathbf{e}_i;\quad \varepsilon\left(\mathbf{r}+a\mathbf{e}_i\right)=\varepsilon\left(\mathbf{r}\right);\quad \sigma\left(\mathbf{r}+a\mathbf{e}_i\right)=\sigma\left(\mathbf{r}\right). \tag{2}$$

Integration of the local strain and stress fields gives the macroscopic, or effective, stiffness tensor $\mathbf{C}^*$ defined as

$$\langle\sigma\rangle=\mathbf{C}^*:\langle\varepsilon\rangle \tag{3}$$

In all considered below test cases, the elastic constants of matrix and fiber materials are taken after [9]: $\nu_0 = 0.35$, $\nu_1 = 0.22$ and $\mu_1/\mu_0 = 44.2/2.39$.

3 Perfect interface: peak stress statistics

Under assumption of perfect interface bonding, the stated boundary-value problem can be solved either numerically [16,17] or analytically [7] for the local stress field. Here, we focus on the interface stress concentration, or normalized peak stress, $s_m = \max\limits_{0\le\varphi<2\pi}\sigma_{rr}/P$ responsible for the interface damage due to uniaxial tension $\langle\sigma\rangle = P\mathbf{e}_2\mathbf{e}_2$. For the ordered sample $s_m^{(q_1)} \le s_m^{(q_2)} \le \ldots \le s_m^{(q_N)}$ obtained from the numerical experiment, we define the empirical cumulative probability function

$$\widehat{F}(\sigma)=\Pr\left[s_m^{(q_i)}<\sigma\right]=(i-0.5)/N \tag{4}$$

Here, $s_m^{(q_i)}$ means a normalized peak stress at the interface between matrix and q_ith fiber. To obtain the test-independent data, $s_m^{(q_i)}$ were averaged over 50 runs at a given fiber volume content c. The empirical probability function (4) obtained by computer simulations for $0 \le c \le 0.5$ is shown in Fig. 2.

Numerical study shows that there always (regardless of c) exists a relatively low fraction of fibers with high interface stress. The max stress is usually localized between the closely placed fiber pairs and exceeds greatly the mean stress value. It means that debonding onset in these spots is most probable. It was found elsewhere [7] that the peak interface stress distribution in composite with uniform random arrangement of fibers follows Fréchet rule

$$F(\sigma)=\exp\left\{-\left[p_3/\left(\sigma-p_1\right)\right]^{p_2}\right\} \tag{5}$$

where $p_i = p_i(c)$ [7]. Below, we take $F(\sigma)$ as an analytical form of the probability function $\Pr\left[s_m<\sigma\right]$.

4 Imperfect interface: numerical approach

Numerical simulation of interface debonding uses the non-linear contact problem where the matrix-fiber interaction is described by the cohesive zone model (CZM) [5]. Specifically,

we adopt the bi-linear CZM [10] relating the normal stress σ_n to normal opening u_n:

$$\sigma_n(u_n) = \begin{cases} K_n u_n, & u_n < u_0 \\ K_n u_n(1-d), & u_0 < u_n < u_c \\ 0, & \text{otherwise.} \end{cases} \tag{6}$$

It comprises the linearly elastic segment with initial contact stiffness K_n and the linear degradation segment with reduced contact stiffness $K_n(1-d)$, $d(u_n)$ being the damage parameter. The max contact stress $\sigma_n(u_0) = \sigma_c$ is called the cohesive strength. An interface damage begins in the point $u_n = u_0$ and ends in the point $u_n = u_c$, where the traction at the newly created crack surface vanishes. The triangle area equals the critical normal mode fracture energy (crack opening work) $G_c = \sigma_c u_c/2$. In fact, this criterion combines the fracture stress and energy conditions for the normal (mode I) crack opening. For the mode II shear stress, the $\sigma_t(u_t)$ relationship is analogous to (6) [10]. For more discussion on the problem statement, see [5].

In order to illustrate CZM capability to model an interface crack onset and propagation, we consider two fibers embedded in an infinite matrix. The uniaxial far tension P is applied in x_2-axis direction; here and below, all the stresses are scaled by σ_c. The stress field evolution and interface crack onset and growth is clearly seen from the Figs 3a - 3d, where the max principal stress σ_1 field is shown for P varying from 0.25 to 1.0. To make the crack opening visible, the displacements are magnified. At the initial stage of loading, the local stress concentration spot lies between the fibers, Fig. 3a. However, already at $P = 0.50$ (Fig. 3b) we observe two distinct stress concentration points which would become the crack tips soon and at $P = 0.75$ (Fig. 3c) we get an open crack. After the defined by the crack tips central angle reached the critical value of ˜$2\pi/3$ ($P = 0.90$, Fig. 3d), the crack stops, in accordance with theory [9]. As seen, the crack nucleation is rather sensitive to the stress field fluctuations. In high-filled composite, the interface stress concentration due to fiber-fiber interaction is expected to govern a place of interface crack onset. This proves using the multi-inclusion model to be pre-requisite for a reliable prediction of progressive debonding in fibrous composite.

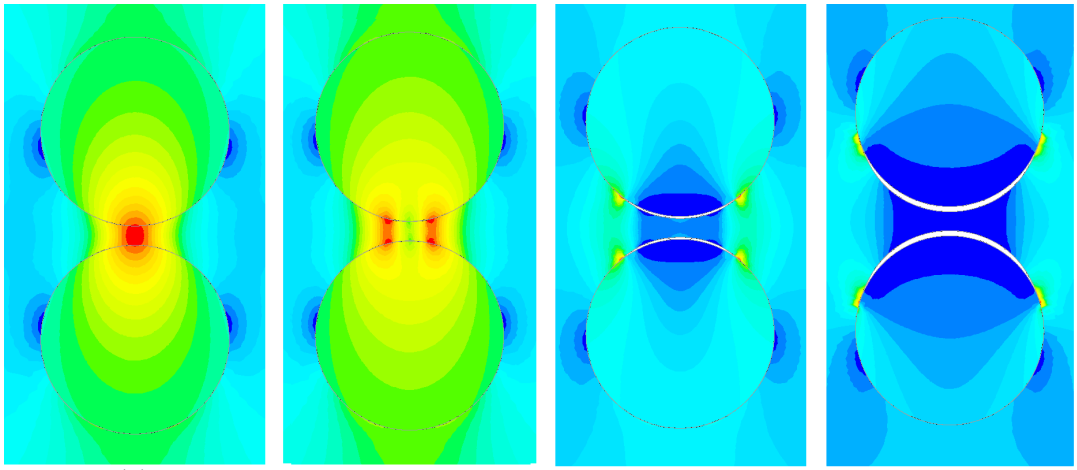

Fig. 3. Effect of fiber interaction on the interface crack onset: $P = 0.25$ (a), 0.50 (b), 0.75 (c) and 0.90 (d)

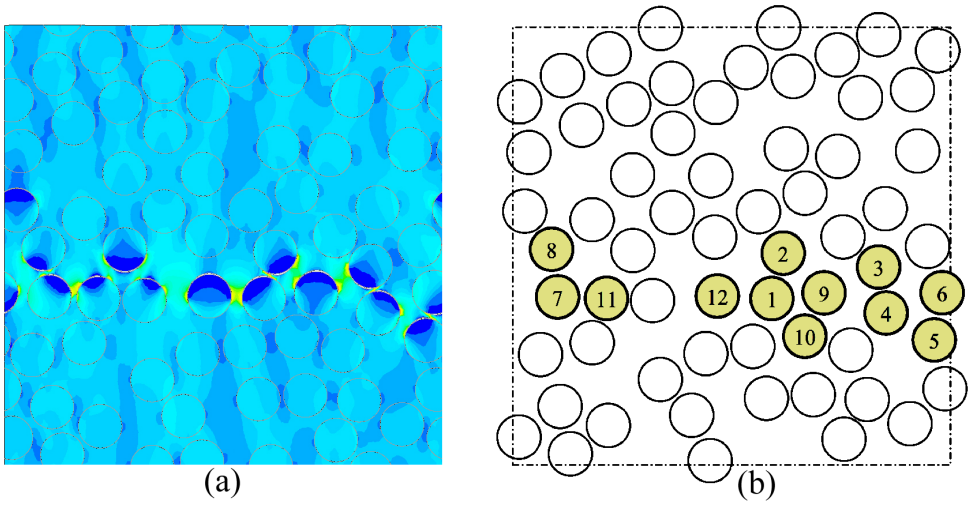

Fig 4. Crack cluster formation in the random structure RUC: (a) numerical solution; (b) analytical solution

Now, we perform analogous numerical experiment for RUC model of composite (Fig. 1) containing $N = 64$ fibers with $c = 0.5$. The boundary conditions are taken in the form (2), the far load is uniaxial strain $\langle\varepsilon\rangle = E\mathbf{e}_2\mathbf{e}_2$. Simulation shows that at the first stage of loading (up to $E = 0.005$), the isolated cracks and crack pairs appear between the fibers with the highest local peak interface stress. The interface cracks cause stress relaxation around these fibers and re-direct some part of total load to the nearest neighbors. This creates favorable conditions for the crack nucleation on these fibers and, as a result, a chain of interface cracks starts to develop at $E = 0.006$. At the last loading step (Fig. 4a), $E = 0.007$. Noteworthy, the crack cluster is oriented across the loading direction, in accordance with experiment [1]. Yet another useful obsrevation consist in that each new crack develops (a) in the point of max interface stress and (b) due to small far load increment. This allows to simplife the simulation procedure by applying an analytical approach that dramatically reduces the computational effort.

5 Imperfect interface: analytical approach

Here, we use an analytical, multipole expansion type solution for RUC model [4] derived under assumption of the open-crack interface model. The interface boundary conditions are:

$$\big[[u]\big]_{L_{qb}} = \big[[T_r]\big]_{L_{qb}} = 0, \quad T_r\Big|_{L_{qs}} = 0, \;\; q = 1, 2, \ldots, N. \tag{7}$$

where $\mathbf{T}_r = \sigma_{rr}\mathbf{e}_r + \sigma_{r\theta}\mathbf{e}_\theta$ is the traction vector at the circular interface L_q. In (7), $\big[[f]\big]_L = f\big|_{L_+} - f\big|_{L_-}$ denotes the function f jump through the interface L, L_+ and L_- being the matrix and fiber sides of interface L, respectively.

Following [4], we write the displacement in a vicinity of the partially debonded fiber in the form

$$2\mu_j\; u_j(\zeta) = \varkappa_j\varphi_j(\zeta) - \left(\zeta - \frac{1}{\overline{\zeta}}\right)\overline{\varphi_j'(\zeta)} - \omega_j\left(\frac{1}{\overline{\zeta}}\right), \tag{8}$$

$j = 0$ for matrix and $j = 1$ for fiber. The potentials φ_j and ω_j in (8) are taken in the form

$$\varphi_0(\zeta) = \frac{(1-\alpha)}{2}f(\zeta) + \frac{(1-\beta)}{2}h(\zeta)R_\lambda(\zeta); \tag{9}$$

$$\omega_0(\zeta) = -\frac{(1-\alpha)}{2} f(\zeta) + \frac{(1+\beta)}{2} h(\zeta) R_\lambda(\zeta);$$
$$\varphi_1(\zeta) = \frac{(1+\alpha)}{2} f(\zeta) + \frac{(1+\beta)}{2} h(\zeta) R_\lambda(\zeta);$$
$$\omega_1(\zeta) = -\frac{(1+\alpha)}{2} f(\zeta) + \frac{(1-\beta)}{2} h(\zeta) R_\lambda(\zeta).$$

Here,

$$\alpha = \frac{\mu_1(\varkappa_0+1) - \mu_0(\varkappa_1+1)}{\mu_1(\varkappa_0+1) + \mu_0(\varkappa_1+1)}, \quad \beta = \frac{\mu_1(\varkappa_0-1) - \mu_0(\varkappa_1-1)}{\mu_1(\varkappa_0+1) + \mu_0(\varkappa_1+1)} \tag{10}$$

are known as the Dundurs' bi-material constants,

$$R_\lambda(\zeta) = (\zeta - \zeta_d)^{\frac{1}{2}+\mathrm{i}\lambda} (\zeta - \overline{\zeta_d})^{\frac{1}{2}-\mathrm{i}\lambda}, \tag{11}$$

$f(\zeta)$ and $h(\zeta)$ are the analytical functions to be found. In (11), $\zeta_d = \exp(i\theta_d)$ and $\lambda = -\log\left(\frac{1-\beta}{1+\beta}\right)/2\pi$. The boundary conditions (7) are fulfilled exactly provided the potentials φ_j and ω_j taken in the form (9).

For the details of solution, see [4]; we note only that the obtained solution provides a study of the stress concentrations, the stress intensity factors and energy release rate at the interface crack tips in FRC and the effective stiffness tensor of composite as a function of volume content and arrangement of fibers and loading type. Here, we apply this solution to model progressive interface debonding by means of simple iterative scheme. First, the RUC model problem is solved under assumption that all the fibers perfectly bonded with matrix. Next, we evaluate local stress field and look for a point where the interface debonding stress criterion [8] $K = (\max(\sigma_n, 0)/\sigma_c)^2 + (\tau_n/\tau_c)^2$ reaches a maximum. Here, σ_c and τ_c is the tensile and shear interface strength, respectively; for simplicity, we take $\sigma_c = \tau_c$. Then, we modify the model by adding the interface crack of fixed length $2\pi R/3$ centered in this point and solve the problem again, etc. The cluster of debonded fibers generated with aid of the modified algorithm is shown in Fig. 4b. Noteworthy, these data are quite similar to those obtained from the finite element study. Comparison shows that all the partially debonded fibers predicted by the analytical model (Fig. 4b), excluding only that one with #10, are predicted also by the numerical, CZM based model (Fig. 4a).

6 Stiffness reduction due to damage accumulation

The numerical approach allows to study the debonding-induced macroscopic stiffness degradation and macroscopic anisotropy of fibrous composite as well. The FRC stress-strain curves obtained from this model is shown in Fig. 5: they are similar to those reported recently in [6] and [11]. Recall, the matrix and fibers are linearly-elastic, so the non-linear behavior of composite is entirely due to progressive interface damage. No irreversible strain is expected: unloading is elastic, with reduced Young modulus (dash-dotted lines in Fig. 5). In view of (3), these data can be used to estimate the effective stiffness C^*_{2222} as the $\langle \sigma_{22} \rangle / \langle \varepsilon_{22} \rangle$ ratio. To get the effective stiffness as a function of crack density, we need to monitor N_{db} (number of partially cracked fibers inside the cell) variation in the course of loading as well.

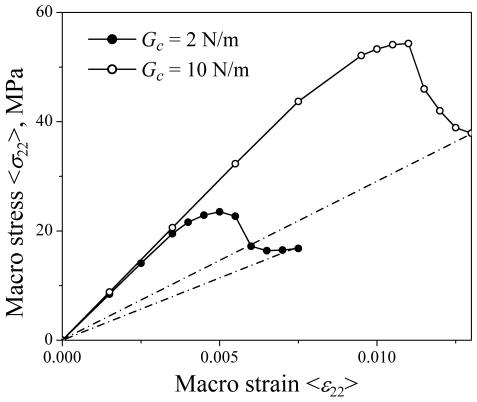

Fig. 5. Elastic stiffness reduction due to interface debonding

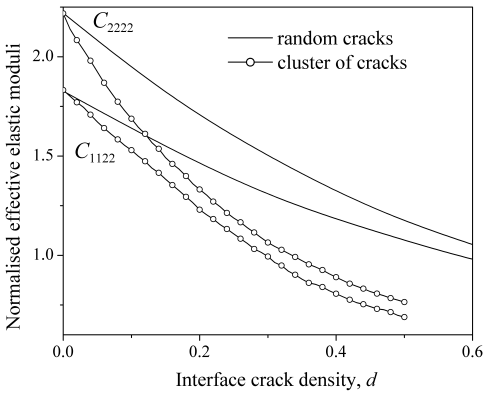

Fig. 6. Effective stiffness: The effect of interface crack density and clustering

Now, we estimate the effect of interface crack density $d = N_{db}/N_p$ on the effective elastic moduli of composite. In the analytical algorithm, the effective elastic moduli (3) are given by simple exact formulas [4] and we re-calculate them at each step, after adding the next crack(s). In order to get the statistically meaningful data, the $C^*_{ijkl}(d)$ values were averaged over 20 runs. As seen from Fig. 6, the effective elastic moduli are substantially affected by the interface crack density d. As computations show, clustering of cracks greatly amplifies FRC stiffness loss in the direction of loading. The moduli C^*_{1122} and C^*_{2222} in the case of stress-induced interface cracks (open circles) are equal to 1.50 and 1.70, respectively, for $d = 0.1$ and 1.23 and 1.36 for $d = 0.2$. The same moduli of composite with uniformly distributed cracks are shown by the solid curves. In particular, they are equal to 1.65 and 1.96, respectively, for $d = 0.1$ and 1.48 and 1.71 for $d = 0.2$. The conclusion drawn from this study that clustering the interface cracks greatly reduces the effective stiffness in the loading direction and increases the damage-induced elastic anisotropy of fibrous composite.

7 Continuum damage model

Practical significance of the developed models consists in that they provide a theoretical background for the continuum theories of composite strength. We consider a simplest theory of this kind to show how available statistical information can be incorporated into the continuum damage model. Specifically, we assume that (a) matrix-fiber interface is the *weakest link* and (b) debonding is the *only* micro damage type. Damage criterion is taken in the form $s_m = \sigma_c/P$, where σ_c is an interface strength: $\sigma_c = \text{const}$ for brittle fracture and $\sigma_c = \sigma_c(N_f)$ for a fatigue, N_f being a number of loading cycles. An elementary damage event is the interface crack appearance so we can consider interface crack density d as a scalar macro parameter of damage.

Now, we recognize that N_{db} is a number of fibers with $s_m \geq \sigma_c/P$. Provided N sufficiently large,

$$d = N_{db}/N \approx \Pr\left\{s_m \geq \sigma_c/P\right\} = 1 - F(\sigma_c/P), \tag{12}$$

where F is defined by (5). This formula gives an expression of damage level in terms of applied load $\langle \sigma_{22} \rangle = P$ and interface strength σ_c. E.g., assuming interface degradation

due to cyclic loading, one can write the damage accumulation rule as

$$d\left(N_f, P, c\right) = 1 - \exp\left\{ - \left[\frac{p_3(c)}{\sigma_c(N_f)/P - p_1(c)} \right]^{p_2(c)} \right\}. \tag{13}$$

It should be noted that (12) and (13) imply that d is sufficiently low and interactions between the cracks is neglected. I.e., this model describes an early stage of interface damage development, characterized by rapid stiffness reduction [1]. For low d, an effect of interface cracks on the overall stiffness loss can be estimated using the data in Figs 5 and 6. For larger d, where interaction and clustering of cracks becomes a dominant factor, the more advanced continuum damage theories involving the the tensorial measure of damage [12] can be developed with aid of the above micromechanical models.

References

[1] Tsai S.W. Composites Design., Think Composites, Dayton, Ohio, 1988.

[2] Shokrieh M.M., Lessard L.B. Progressive fatigue damage modeling of composite materials. Part I: modeling. J. Compos. Mater. 2000, 34, 1056–1080.

[3] Ghosh S., Ling Y., Majumdar B., Kim R. Interfacial debonding analysis in multiple fiber reinforced composites. Mech. Mater., 2000, 32, 561-591.

[4] Kushch V.I., Shmegera S.V., Mishnaevsky L. Jr. Elastic interaction of partially debonded circular inclusions. II. Application to fibrous composite. Int. J. Solids Struct. 2011, 48, 2413–2421.

[5] Kushch V.I., Shmegera S.V., Mishnaevsky L. Jr. Numerical simulation of progressive debonding in fiber reinforced composite under transverse loading. Int. J. Eng. Sci., 2011, 49, 17-29.

[6] Romanowicz M. Progressive failure analysis of unidirectional fiber-reinforced polymers with inhomogeneous interphase and randomly distributed fibers under transverse tensile loading. Composites A, 2010, 41, 1829-1838.

[7] Kushch V.I., Shmegera S.V., Mishnaevsky L. Jr. Meso cell model of fiber reinforced composite: interface stress statistics and debonding paths. Int. J. Solids Struct. 2008, 45, 2758-2784.

[8] Ha S.K., Jin K.K., Huang Y. Micro-mechanics of failure (MMF) for continuous fiber reinforced composites. J. Compos. Mater. 2008, 42, 1873-1895.

[9] Toya M. A crack along interface of a circular inclusion embedded in an infinite solid. J. Mech. Phys. Solids 1974, 22, 325-348.

[10] Alfano G., Crisfield M.A. Finite element interface models for the delamination anaylsis of laminated composites: mechanical and computational issues. Int. J. Numer. Meth. Eng., 2001, 50, 1701-1736.

[11] Vaughan T.J., McCarthy C.T. Micromechanical modelling of the transverse damage behaviour in fibre reinforced composites, Compos. Sci. Technol., 2011, 71, 388–396.

[12] Ju J.W. A micromechanical damage model for uniaxially reinforced composites weakened by interfacial arc microcracks. ASME J Appl. Mech., 1991, 58, 923–930.

Volodymyr I. Kushch, Institute for Superhard Materials of the National Academy of Sciences of Ukraine 2, Avtozavodskaya St., 04074, Kiev, Ukraine